

# DKCDF: Dual-Kernel CNN with Dual Feature Fusion for Lung Cancer Detection

Wariyo G. Arero<sup>1</sup><sup>a</sup>, Yaqin Zhao<sup>1</sup><sup>b</sup>, Longwen Wu<sup>1</sup><sup>c</sup> and Yi Wang<sup>2</sup>

<sup>1</sup>*School of Electronics and Information Engineering, Harbin Institute of Technology, Harbin, China*

<sup>2</sup>*Fushan Environmental Monitoring Center, Yantai, China*

**Keywords:** Multi Feature Fusion, CNN, Lung Cancer, HOG, LBP.


**Abstract:** One of the main reasons for cancer-related fatalities worldwide is lung cancer. Early diagnosis is essential for enhancing patient outcomes and lowering mortality rates. Deep learning-based approaches have recently demonstrated promising outcomes in medical image analysis applications, such as lung cancer identification. In order to improve lung cancer detection, this research suggests a unique method that combines a dual-kernel convolutional neural network (DKC) with dual-feature fusion using the Histogram of oriented gradients (HOG) and local binary patterns (LBP). Convolutional neural networks are good at extracting and detecting features. CNN features are built using low-level features from the first convolution layer, which might only partially capture some local features and lead to the loss of some crucial details like edges and contours. HOG is quite good at describing the shape of objects. LBP can record local structure and information about spatial texture. The distribution of edge directions or local gradients in intensity can provide a good definition of an object's shape and local appearance. The lung image is loaded with bone, air, blood, water and other substances and appears noisy in the lung image. As a result, in this research, we favor the HOG and LBP feature fusion for lung cancer detection.


## 1 INTRODUCTION


The prognosis of patients who have lung cancer can be significantly improved by early identification, which is a primary global health concern. The manual analysis of medical pictures used in traditional lung cancer screening procedures can be time-consuming and prone to human error. Therefore, it is crucial to create automated and reliable lung cancer detection technologies. In recent times, the convergence of computer vision and medical imaging has become a promising frontier in the pursuit of diagnostic tools that are both more accurate and efficient (Han et al., 2019; Liang et al., 2023). Within this realm, the amalgamation of dual kernel techniques, along with the integration of various features like Histogram of Oriented Gradients (HOG) and Local Binary Patterns (LBP), has demonstrated significant promise in elevating the sensitivity and specificity of systems designed for detecting lung cancer. In this study, we

introduce a dual-kernel CNN-based method for improving lung cancer detection by combining HOG and LBP characteristics.

Cancer is characterized by the uncontrolled growth of cells in the body, with lung cancer specifically involving the formation of malignant cells within the lungs. Especially in developing nations, it stands out as the most prevalent cancer among both men and women and the second most frequently diagnosed disease. The main contributors to lung cancer are believed to be smoking, exposure to air pollution, and insufficient nutrition. Globally, the number of lung cancer cases and deaths has considerably grown (Bade & Cruz, 2020). Annually, the American Cancer Society provides estimates for new cancer cases and deaths in the United States by compiling the latest data on population-based cancer occurrences and outcomes. This information is derived from incidence data gathered by central cancer registries and mortality data collected by the

<sup>a</sup> <https://orcid.org/0009-0001-9074-4948>

<sup>b</sup> <https://orcid.org/0000-0002-0167-0597>

<sup>c</sup> <https://orcid.org/0000-0002-6914-6695>

National Center for Health Statistics. For the year 2023, it is projected that there will be 1,958,310 new cancer cases and 609,820 cancer-related deaths in the United States (Siegel, Miller, Wagle, & Jemal, 2023). As scientists explore the complexities of medical imaging, the need for advanced algorithms capable of discerning meaningful patterns from intricate datasets has surged (Ma, Wan, Hao, Cai, & Liu, 2023). The dual-kernel approach, a robust concept in machine learning, entails utilizing multiple kernels to capture varied facets of data representation. This paper centers on the utilization of the dual-kernel methodology within the realm of lung cancer detection, seeking to harness the complementary information inherent in different feature spaces.

A critical element of our proposed approach revolves around merging two distinct texture descriptors, namely HOG and LBP. The HOG descriptor excels at capturing the spatial arrangement of pixel intensities, emphasizing gradient information crucial for delineating structural nuances in medical images. Conversely, LBP, renowned for its ability to encode local texture patterns, contributes a supplementary layer of information, enhancing the overall feature representation.

The rationale behind this fusion strategy is grounded in the notion that different imaging modalities may highlight diverse aspects of the underlying pathology. By combining the strengths of HOG and LBP within a dual kernel framework, our goal is to construct a more comprehensive and discriminative feature set, thereby bolstering the robustness of our lung cancer detection system.

Additionally, the diagnosis is typically made at an advanced stage, when there is no longer hope for treatment (Soerjomataram et al., 2023). In order to enhance overall survival, detect lung cancer in its earliest stages while successful therapies are still viable, and lower side effects associated with systemic treatments, it is vital to develop novel diagnostic techniques that boost the accuracy of early diagnosis (Shah, Malik, Muhammad, Alourani, & Butt, 2023). Examining computed tomography (CT) images is one of the crucial steps in the pre-diagnosis of lung cancer. The pre-diagnosis process that follows X-ray or Computed Tomography (CT) scanning takes the radiologist a lot of time and energy. Additionally, this scanning procedure calls for a very high level of focus and proficiency. In particular, if interpretation is heavily reliant on prior expertise, less experienced radiologists have extremely variable detection rates, which accelerates the speed of false positive detection (S. Shen, Han, Aberle, Bui, & Hsu, 2019).

Low-dose helical Computed Tomography (LDCT) (Fang Lei, 2019) (Fedewa et al., 2021) is currently being used as a method for lung cancer screening (Jonas et al., 2021). To increase the diagnostic accuracy for the classification of lung cancer detection, several efforts are being made to develop computer-assisted diagnosis and detection systems. The development of computer-aided systems was motivated by the requirement for trustworthy and impartial analysis. The purpose of this research is to identify whether a picture is cancerous or not and to extract features for detection (Ani Brown Mary & Deje, 2018).

The identification, segmentation, and classification of benign and malignant pulmonary nodules are the core topics of research on deep learning-based lung imaging approaches. To enhance the performance of deep learning models, researchers mainly concentrate on creating new network architectures and loss functions. Review papers on deep learning approaches have lately been published by a number of research groups (Mandal & Vipparthi, 2021) (Hamedianfar, Mohamedou, Kangas, & Vauhkonen, 2022) (Highamcatherine & Highamdesmond, 2019). However, deep learning techniques have advanced quickly, and every year, numerous new approaches and applications appear. This study has topics that earlier studies were unable to cover.

Early detection of lung cancer patients can considerably improve their prognosis, which is a serious global health concern. Traditional lung cancer screening methods include the manual examination of medical images, which can be time-consuming and prone to human error. Therefore, developing automated and trustworthy lung cancer detection methods is essential. In this article, we combine the HOG and LBP feature fusion mechanisms to present a dual-kernel CNN-based technique for enhancing lung cancer identification. The following is our work's primary contribution:

1. We propose dual paths CNN with different receptive fields (dual-kernel).
2. We propose that HOG and LBP features are fused with the output of our dual-kernel CNN to supplement the edge, profile information and spatial texture information of lung images.
3. We fix the problem of class imbalance by using data augmentation.

In the subsequent sections, we delve into the technical foundations of our methodology, which involves dual kernels and the fusion of multiple features. We illustrate its potential through experimental results and comparative analyses. As we

navigate through the intricacies of this innovative approach, it becomes evident that the amalgamation of diverse features and dual kernel processing not only enhances the accuracy of lung cancer detection but also provides a more nuanced understanding of the disease at the pixel level. To conclude, this paper introduces an innovative advancement in medical image analysis by highlighting the effectiveness of a dual kernel framework combined with the fusion of HOG and LBP features for improved lung cancer detection. Our study emphasizes the significance of harnessing diverse information sources and showcases how advanced machine learning techniques have the potential to reshape the landscape of early cancer diagnosis.

The remainder of this paper is organized as follows: we describe related works in part 2, the method and dataset in part 3, next experiment in part 4, ablation study in part 5 and finally conclusion in part 6.

## 2 RELATED WORK

Image processing methods have been studied in the past to detect lung cancer (Gurcan et al., 2002). The field of medical imaging has recently seen the adoption of neural networks and deep learning techniques (Fakoor, Ladhak, Nazi, & Huber, 2013) (Greenspan, Van Ginneken, & Summers, 2016) (D. Shen, Wu, & Suk, 2017). In order to categorize and diagnose lung cancer using machine learning and neural networks, a number of researchers (Cai et al., 2015) (Al-Absi, Belhaouari, & Sulaiman, 2014) (Gupta & Tiwari, 2014) (Penedo, Carreira, Mosquera, & Cabello, 1998) (Taher & Sammouda, 2011) (Kuruvilla & Gunavathi, 2014) have made an effort. Deep learning methods have not been used frequently to identify lung cancer. This is due to the dearth of a sizable dataset of medical photographs, particularly those of lung cancer. Urine samples are used by Shimizu et al. (Shimizu et al., 2016) to identify lung cancer.

When the literature is searched, a sizable number of research are discovered that help with the quick detection of lung cancer. Wang and colleagues (Wang et al., 2018) suggested a new CNN-based methodology to categorize cancerous or non-cancerous tissue. In the suggested model, full-slide imaging (WSI) is typically one megapixel. Hence, considerably smaller picture patches recovered from WSI are frequently employed as input. Each 300x300 pixel image patch from lung adenocarcinoma (ADC) WSIs was employed in this 2018 study. The suggested model had a success percentage of 89.8%.

A deep convolutional neural network-based pulmonary nodule identification technique is proposed by Deng and Chen (DENG & CHEN, 2019), which ingeniously includes the deep supervision of incomplete CNN layers. (S. Chen, Han, Lin, Zhao, & Kong, 2020) uses balanced CNN with traditional candidate detection to create a computer-aided detection (CADE) strategy. A convolutional neural network-based automatic pulmonary nodule identification and classification system with only four convolutional layers is proposed by Masud et al. (Masud et al., 2020).

The DSC (dice coefficient) for nodule segmentation is 73.6%, according to Tong et al.'s (Tong, Li, Chen, Zhang, & Jiang, 2018) proposed pulmonary nodule segmentation algorithm, which is based on an upgraded U-Net and adds a residual network.

(Guo et al., 2014) suggests using a convolution neural network to create a lung cancer prediction system, which resolves the problems with manual cancer prediction. During this procedure, CT scan images are gathered and processed using a layer of neural network that automatically extracts image features. These features are then processed using deep learning to predict the features associated with cancer using a large volume of images.

The system the authors developed assists in decision-making while analysing the patient's CT scan report. With the aid of convolution neural networks, lung nodules from CT scan pictures were predicted (El-Baz et al., 2013). In order to effectively classify lung cancer-related features as benign and malignant, LIDC IDRI database images are gathered and put into the stack encoder (SAE), convolution neural network (CNN), and deep neural network (DNN). A technique developed by the author provides an accuracy of up to 84.32%. In our work, we introduce dual-kernel CNN, which is used for local and global range dependencies because most deep learning networks are limited to fixed receptive field size; we also propose a feature fusion mechanism, which is HOG and LBP, which are used for obtaining more comprehensive lung feature and improve the ability to describe and identify lung cancer image.

## 3 METHODS

### 3.1 Data Set and Pre-Processing

We take advantage of the Kaggle Data Science Bowl 2017 (KDSB, 2017) (Kaggle, 2017) database of medical images. The data set includes 2101 images that have been labelled with 0 for patients without

cancer and 1 for patients with cancer. Digital Imaging and Communications in Medicine, or DICOM, is the format used for the image. This dataset has a label of 0 for 70% of the data and a label of 1 for the remaining 30%. The CT scan for each patient consists of a variable number of images (often 100–400; each image is a 2-D axial slice) with a resolution of 512x512 pixels. Nodules in this dataset are not labelled.

Due to tumours in the lung tissue, the lung image consists of unimportant parts that must be removed through segmentation. These unimportant parts include bone, air, blood, water, and other substances that must be excluded due to their effects on data noise and nodule learning. The Hounsfield (HU), a unit of radio density and representative of CT scan radio densities, is the measurement used in CT scans. Diverse researchers employ several segmentation techniques to weed out irrelevant data, including clustering (Rao, Pereira, & Srinivasan, 2016), k-means (Gurcan et al., 2002), watershed (Ronneberger, Fischer, & Brox, 2015), and thresholding (Alakwaa et al., 2017). In our work, we used thresholding with a filter value of -600 to our 2D image.

Initially, the pixel values of each CT scan are transformed into Hounsfield Units (HU), a quantitative metric used to express the radio density of substances in lung CT images. Notably, the lung, bone, blood, kidney, and water exhibit radio density values of -500 HU, 700 HU, 0 HU, 30 HU, and 0 HU respectively. Following this conversion, each CT scan comprises multiple slices, with pixel values corresponding to HU and falling within the range of [-1024, 3071].

Table 1: Typical Radio densities in HU of Various Substances in a CT scan (Alakwaa, Nassef, & Badr, 2017).

Substance	Radio density(HU)
Air	-1000
Lung tissue	-500
Water and Blood	0
Bone	700

The subsequent step involves the removal of specific tissues, a process commonly addressed by scholars through methods described above. In our study, we opt for thresholding. To accomplish this, a Gaussian filter is applied, and pixel values are normalized to fit within the [0, 1] range, utilizing a threshold of -600. Figure 2 depicts a CT scan slice of a patient alongside its segmentation outcome based on thresholding.

To enable the utilization of the proposed network, we convert the HU values of each slice into UINT8, signifying that the initial raw data, ranging from [-1024, 3071], undergo linear transformation to [0, 255]. Subsequently, the mask employed for lung tissue segmentation is multiplied by these values, with substances outside the mask set to 170, representing a standard tissue luminance.

We used the thresholding technique to segment the CT scan image. The unnecessary parts of the lungs with their typical radio densities of different parts of the CT scan are shown in Table 1; as shown in Table 1, the pixels near -1000 and greater than -320 are masked. The resampled image with thresholding -600 of sample patients with 3D plotting is shown in Figure 2.

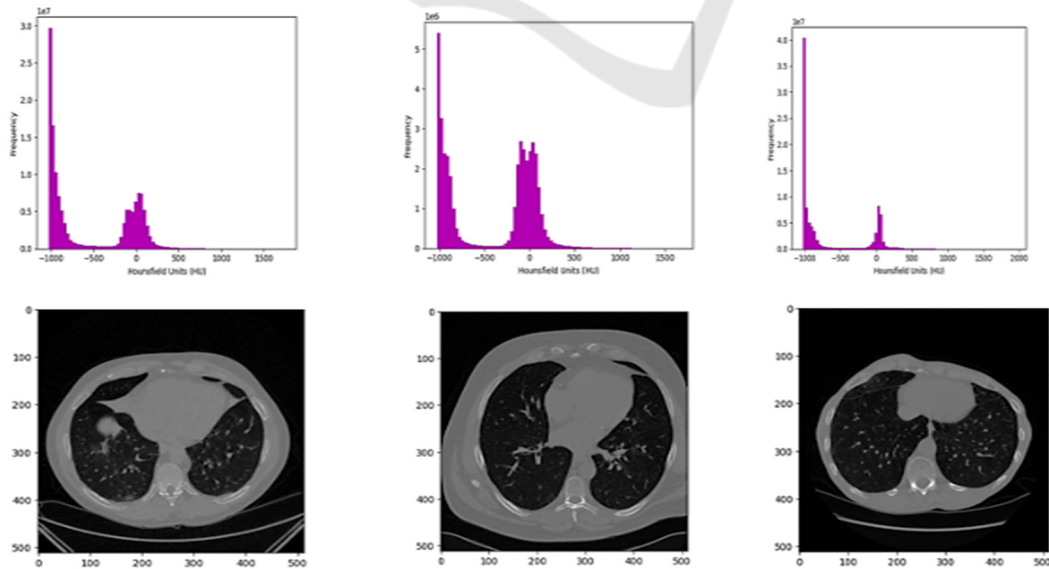


Figure 1: Histogram of pixel values in HU (Hounsfield) for patient 601 at 180 slices, patient 801 at 70 slices, and patient 1001 at slice 120, respectively and with corresponding 2D axial.



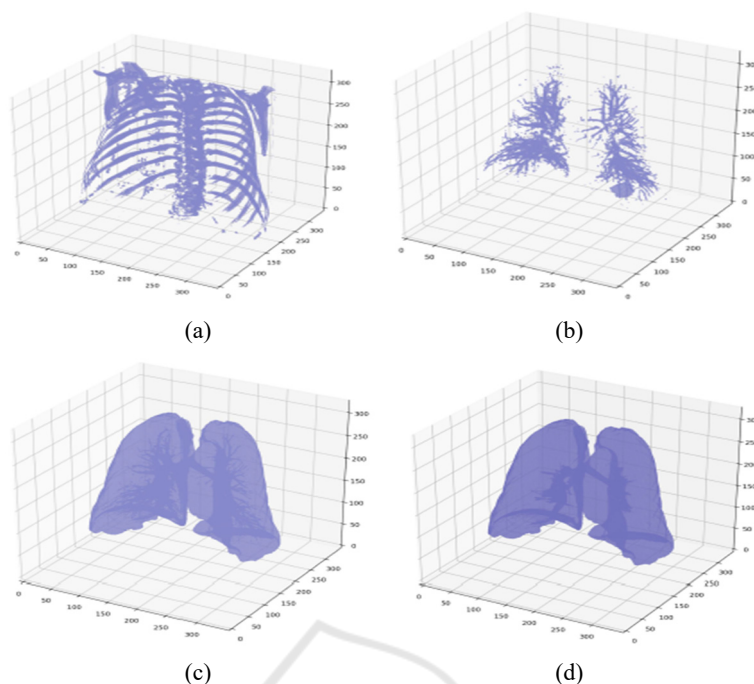


Figure 2: 2(a) resample of a 3D image with 600-pixel value HU uncover the bone segment 2(b) resample of sample patient including lung bronchioles 2(c) resample sample patient performing mask with air 2(d) resample sample patient with bronchioles included as a terminal mask.

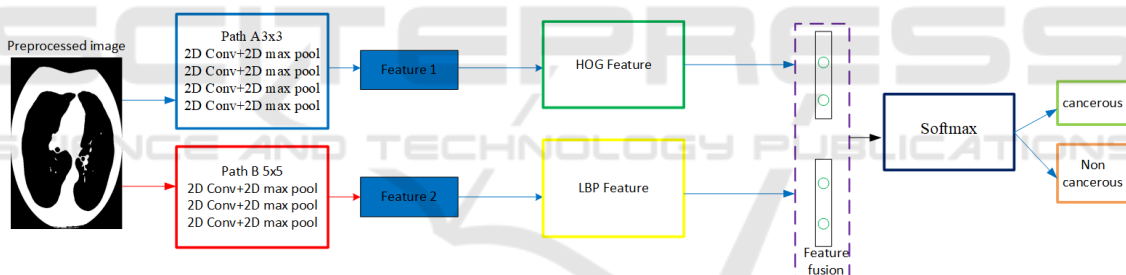


Figure 3: Our proposed dual-kernel with dual-feature fusion model.

### 3.2 Dual-Kernel CNN

Because most researchers only use one receptive field within a single path, this affects the nearby pixel and high-level information during feature extraction. To address this challenge, we propose two dual CNNs with different receptive field sizes with dual-feature fusion mechanisms. We named our paths as path A and path B with receptive field sizes 3x3 and 5x5, respectively. The output of path A from the fourth convolution layer is concatenated with the first convolution layer of the second path. Path A has four convolution layers and four max pooling layers. Three convolution layers and three maximum pooling layers are present in the second path. We only paid attention to the indicated kernel sizes and two paths.

In order to study the problems described. Table 2 contains the model parameters. Furthermore, in the proposed model, we incorporate a feature fusion strategy. Figure 3 shows the network of the proposed model.

### 3.3 Feature Fusion

The objective of feature extraction is typically to portray the raw data as a condensed set of features that more accurately captures its essential characteristics and attributes. By doing so, we can lower the original input's dimensionality and train pattern recognition and classification algorithms using the new features as input. In our study, we make use of two types of features, HOG and LBP, which we will go through individually below.

### 3.3.1 Histogram of Gradients (HOG) Feature Fusion

The HOG description highlights an object's structure or shape, distinguishing it from the edge features used in photo extraction. While edge features focus solely on determining if a pixel is part of an edge, HOG goes further by providing information on edge direction. This involves extracting gradients and orientations (magnitude and direction) of edges, dividing the entire image into smaller sections, and determining gradients and orientation for each region. Subsequently, HOG generates separate histograms for each zone. The term "Histogram of Oriented Gradients" denotes the histograms produced from pixel values' gradients and orientations. In a dense grid, the HOG approach (Dalal & Triggs, 2005) evaluates locally normalized histograms of image gradient origins, effectively characterizing an object's form and local appearance through edge distribution or local intensity gradients. This method proves valuable in discerning lung characteristics, particularly in identifying lung cancer, as it provides orientation information about the lung boundary and texture details in the surrounding area. The lung, containing extraneous elements like air, bone, tissue, and water in the low-attenuation region, benefits from the nuanced information provided by the HOG feature extraction approach.

The HOG feature extraction method (Dalal & Triggs, 2005) evaluates locally normalized histograms of picture gradient origins in a dense grid. Edge distribution or local intensity gradients can efficiently describe an object's form and local appearance. The lung is filled with extraneous components, including air, bone, tissue, and water and appears in a low-attenuation region. Therefore, the only information offered is orientation information of the lung boundary and texture information of the surrounding area. Therefore, in this study, we favor the HOG characteristic for identifying lung cancer. We show a sample image with HOG feature fusion in Figure 4.

$$\begin{aligned} G_x(r, c) &= I(r, c+1) - I(r, c-1) \\ G_y(r, c) &= I(r-1, c) - I(r+1, c) \end{aligned} \quad (1)$$

After calculating  $G_x$  and  $G_y$ , the magnitude and angle of each pixel are calculated using the formulae mentioned below.

$$\begin{aligned} \text{Magnitude}(\mu) &= \sqrt{G_x^2 + G_y^2} \\ \text{Angle}(\theta) &= \left| \tan^{-1} \left( \frac{G_y}{G_x} \right) \right| \end{aligned} \quad (2)$$

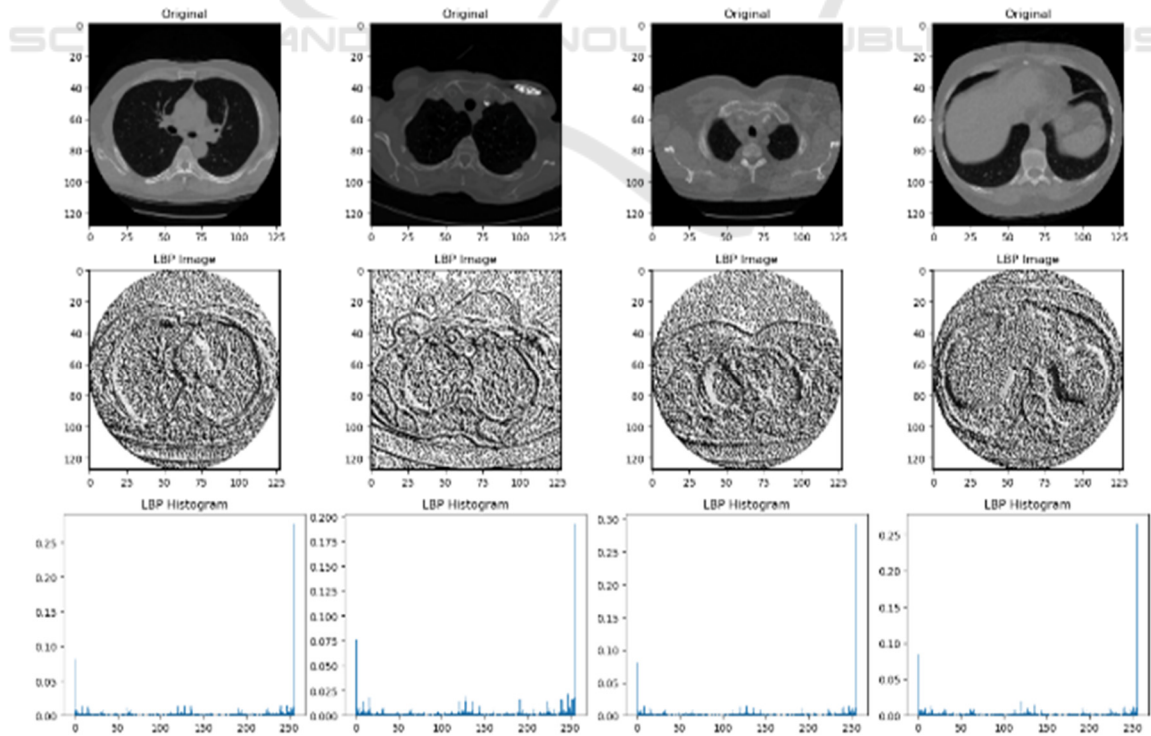


Figure 4: Sample of Lung image by LBP feature with its Histogram.

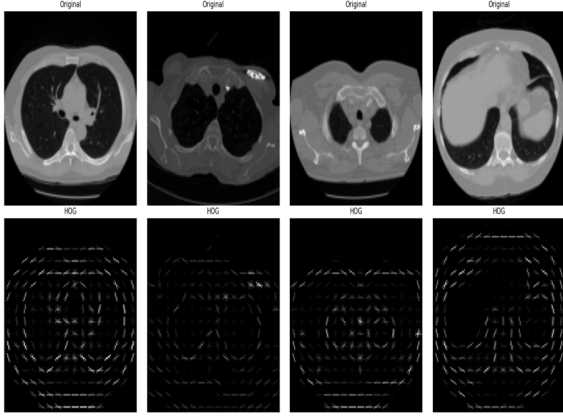


Figure 5: A sample lung image with HOG feature.

### 3.3.2 Local Binary Feature (LBP)

In biomedical image analysis, two-dimensional texture analysis is incredibly crucial. A practical and multiresolution method for processing a grayscale image is LBP (Ojala, Pietikäinen, & Harwood, 1996). It is a rotation-invariant texture descriptor built using nonparametric sample discrimination and local binary patterns. There are two different sorts of distinguishing information for the lung imaging sign: (1) edge orientation and grayscale gradient information and (2) backdrop texture. The edge information of the lung is only auxiliary and generic for class differentiation because the lung itself is packed with extraneous components like air, bone, tissue, water, and other substances. The background information of a lung cancer imaging sign is crucial for its recognition, making the LBP helpful texture for lung cancer diagnosis.

$$LBP_{P,R}(x_c, y_c) = \sum_{p=0}^{P-1} s(g_p - g_c) 2^p \quad (3)$$

$$s(x) = \begin{cases} 1 & x \geq 0 \\ 0 & x < 0 \end{cases} \quad (4)$$

where  $x_c$  and  $y_c$  are the coordinates of the center pixel,  $p$  are circular sampling points,  $P$  is the number of sampling points or neighborhood pixels,  $g_p$  is the grayscale value of  $p$ ,  $g_c$  is the center pixel, and  $s$  or sign is threshold function. For classification purposes, the LBP values are represented as a histogram, as we show in Figure 5.

A variety of applications, including face recognition (Ahonen, Hadid, & Pietikainen, 2006)

and medical picture analysis (Tian, Fu, & Feng, 2008), have made extensive use of the LBP (Ojala et al., 1996), a potent tool for characterizing texture properties. The first LBP operator which was first presented in (Ojala et al., 1996) by Ojala et al. By comparing the points of, for instance,  $3 \times 3$  neighboring pixels with respect to the value of the central pixel, LBP is a straightforward approach that creates binary codes. If the neighboring pixel's value is less than the center pixel's, it produces the binary code 0. If not, it produces the binary code 1. The LBP code is created by multiplying the binary codes by the respective weights and adding the results. This value is determined using Eq. (1) as follows:

$$LBP_{P,R}(x, y) = \sum_{i=0}^{P-1} s(g_i - g_c) 2^i \quad (5)$$

$$S(g_i - g_c) = \begin{cases} 1 & \text{if } g_i \geq g_c \\ 0 & \text{else} \end{cases} \quad (6)$$

Table 2: The parameter of our multi-kernel model.

Path A			
Layers	w. size/ #weight	Activation	Input
Conv	3×3/32	ReLu	128×128×1
Max pool	2×2		32×126×126
Conv	3×3/32	ReLu	32×125×125
Max pool	2×2		32×123×123
Conv	3×3/32	ReLu	32×122×122
Max pool	2×2		32×120×120
Conv	3×3/32	ReLu	32×119×119
Max pool	4×4		32×115×115
Path B			
Conv		ReLu	128×128×1
Max pool	2×2		32×124×124
Conv	5×5/32	ReLu	32×123×123
Max pool	2×2		32×119×119
Conv	5×5/32	ReLu	32×118×118
Max pool	2×2		32×115×115

## 4 EXPERIMENTS

We implement our model by using one of the deep learning library tensors flows with Keras backend, which supports a graphical processing unit (GPU).

This tensor flow backend Keras with GPU speeds up the process of a deep learning algorithm. We describe the parameters of our model, such as kernel size, convolution layer, pooling layer, hidden layer, stride and others, in Table 2. The parameter in the table is the one in which our model achieves the best performance on the validation set. The training hyperparameters, including initial momentum, end momentum, learning rate, and weight decay, were configured as 0.5, 0.8, 0.001, and 0.001, respectively. Stride 1 was applied to convolution and max-pool layers to maintain per-pixel precision. The filters for all layers, except the softmax layer's parameter initialized to the label's log, were randomly initialized from uniform distributions (-0.005, 0.005). Finally, the network's bias was set to zero. We have shown our results in Table 3.

		Predicted class	
		0	1
Actual classes	0	0.986	0.014
	1	0.022	0.978

Figure 6: Confusion matrix of our model.

Table 3: Result achieved from our model.

Accuracy	Precision	Recall	Specificity
98.2%	98.6%	97.8%	98.5%

#### 4.1 Performance Evaluation

Researchers have put up a number of performance evaluations for medical image identification. Accuracy, recall, and specificity are among the metrics that are frequently used. We frequently use performance metrics like accuracy (A), recall (R), precision (P), and specificity (S) to gauge how well our model performs.

Table 4: Contestation of our method with other methods.

Methods	Accuracy	Precision	Recall	Specificity
DCLCCST (Y. Chen et al., 2022)	94.7%	95.6%	93.9%	95.5%
MLBLCDMIF (Nazir, AlQahtani, Jadoon, & Dahshan, 2023)	97.1%	97.8%	96.4%	97.7%
GLCDGM (Salama, Shokry, & Aly, 2022)	97.6%	98.4%	96.8%	98.3%
DKCDF	98.2%	98.6%	97.8%	98.5%

$$A = \frac{(tp + tn)}{(tp + fp + fn + tn)} \quad (7)$$

$$S = \frac{t_n}{t_n + f_p} \quad (8)$$

$$R = \frac{t_p}{t_p + f_n} \quad (9)$$

$$P = \frac{t_p}{t_p + f_p} \quad (10)$$

## 5 ABLATION STUDY

Our suggested lung cancer detection model, which uses a dual-kernel technique with the fusion of two different feature types, Histogram of Oriented Gradients (HOG) and Local Binary Patterns (LBP), conducts an ablation study to examine the influence of individual components. Understanding how each feature type contributes to the performance of the entire model is the primary goal of this study.

For the purpose of detecting lung cancer, our foundational model, known as the dual-kernel with dual-feature fusion, combines both HOG and LBP features. After that, while maintaining the values of all other model elements and hyper parameters, we systematically assess how well the model performs when one of these feature types is removed. Considered are three main experimental conditions:

The combination of dual kernels and multiple features represents our entire model architecture.

In this configuration, we use a dual-kernel with LBP (without HOG) and only LBP features for classification, excluding HOG features from the model.

HOG and dual kernels without LBP Here, we use HOG features for classification and omit LBP features from the model.

With both HOG and LBP features included, the dual-kernel with dual-feature fusion achieves the most remarkable accuracy of 98.2%. This demonstrates how the dual-kernel technique with feature fusion effectively improves the model's performance for detecting lung cancer. The accuracy of the model falls to 96.7% when HOG features are



removed, and only LBP features are used. This shows that HOG characteristics highly influence the model's capacity to identify lung cancer. The accuracy decline (-1.5%) highlights the significance of HOG elements in our model.

Conversely, the accuracy stays high at 97.1% when we do not include LBP characteristics and solely use HOG features. Even while this setup outperforms employing only LBP characteristics, it still falls short of the dual-kernel with dual-feature fusion model. This shows that, although to a lesser extent than HOG, LBP features help offer additional information. Our lung cancer detection model's overall accuracy is improved by both the HOG and LBP features, according to our ablation study. As their removal causes a more significant accuracy loss than the omission of LBP features, HOG features, in particular, are more crucial to improving model performance. The significance of feature fusion and the dual-kernel technique in enhancing the performance of deep learning models for lung cancer detection is therefore highlighted by our research.

Table 5: Result analysis from ablation experiment.

Methods	Accuracy	Precision	Recall	Specificity
DKCDF	98.2%	98.6%	97.8%	98.5%
DKC-HOG	97.1%	97.8%	96.4%	97.7%
DKC-LBP	96.6%	97.0%	96.4%	96.9%

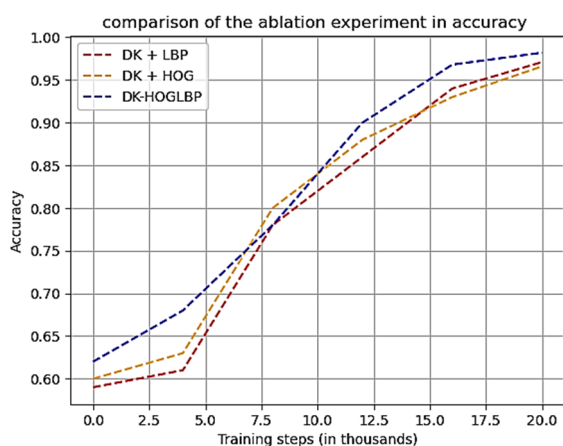


Figure 7: Accuracy graph from the ablation experiment.

## 6 CONCLUSIONS

The article presents an innovative approach to lung cancer detection by employing a dual-kernel with dual-feature fusion method, incorporating Histogram of Oriented Gradient and Local Binary Pattern fusion techniques. Our assessment using the Kaggle Data Science Bowl 2017 (KDSB, 2017) dataset reveals superior outcomes when compared to recent methodologies, highlighting advancements in accuracy, recall, precision, and specificity. To be specific, our model demonstrates an enhancement of 98.2%, 98.6%, 97.8% and 98.5% of accuracy, precision, recall and specificity respectively achieved.

These improved findings emphasize the potential impact of our approach on enhancing lung cancer detection, with implications for early diagnosis and treatment strategies. In our forthcoming research, we aim to investigate transfer learning methods to further refine the accuracy of our proposed model. This strategic approach seeks to leverage the insights gained from our current model and apply them to new data, fostering ongoing enhancements in lung cancer detection.

## ACKNOWLEDGEMENTS

This work is supported by The National Natural Science Foundation of China under Grant Numbers 61671185 and 62071153.

## REFERENCES

Ahonen, T., Hadid, A., & Pietikainen, M. (2006). Face description with local binary patterns: Application to face recognition. *IEEE transactions on pattern analysis and machine intelligence*, 28(12), 2037-2041.

Al-Absi, H.R., Belhaouari, S.B., & Sulaiman, S. (2014). A computer aided diagnosis system for lung cancer based on statistical and machine learning techniques. *J. Comput.*, 9(2), 425-431.

Alakwaa, W., Nassef, M., & Badr, A. (2017). Lung cancer detection and classification with 3d convolutional neural network (3d-cnn). *International Journal of Advanced Computer Science and Applications*, 8(8).

Ani Brown Mary, N., & Dejeu, D. (2018). Classification of coral reef submarine images and videos using a novel z with tilted z local binary pattern ( $z \oplus tzlbp$ ). *Wireless Personal Communications*, 98, 2427-2459.

Bade, B.C., & Cruz, C.S.D. (2020). Lung cancer 2020: Epidemiology, etiology, and prevention. *Clinics in chest medicine*, 41(1), 1-24.

- Cai, Z., Xu, D., Zhang, Q., Zhang, J., Ngai, S.-M., & Shao, J. (2015). Classification of lung cancer using ensemble-based feature selection and machine learning methods. *Molecular BioSystems*, *11*(3), 791-800.
- Chen, S., Han, Y., Lin, J., Zhao, X., & Kong, P. (2020). Pulmonary nodule detection on chest radiographs using balanced convolutional neural network and classic candidate detection. *Artificial Intelligence in Medicine*, *107*, 101881.
- Chen, Y., Feng, J., Liu, J., Pang, B., Cao, D., & Li, C. (2022). Detection and classification of lung cancer cells using swin transformer. *Journal of Cancer Therapy*, *13*(7), 464-475.
- Dalal, N., & Triggs, B. (2005). *Histograms of oriented gradients for human detection*. Paper presented at the 2005 IEEE computer society conference on computer vision and pattern recognition (CVPR'05).
- DENG, Z., & CHEN, X. (2019). Pulmonary nodule detection algorithm based on deep convolutional neural network. *Journal of Computer Applications*, *39*(7), 2109.
- El-Baz, A., Elnakib, A., El-Ghar, A., Gimel'farb, G., Falk, R., & Farag, A. (2013). Automatic detection of 2d and 3d lung nodules in chest spiral ct scans. *International journal of biomedical imaging*, 2013.
- Fakoor, R., Ladhak, F., Nazi, A., & Huber, M. (2013). *Using deep learning to enhance cancer diagnosis and classification*. Paper presented at the Proceedings of the international conference on machine learning.
- Fang Lei, B. (2019). *Barriers to lung cancer screening with low-dose computed tomography*. Paper presented at the Oncology nursing forum.
- Fedewa, S.A., Kazerooni, E.A., Studts, J.L., Smith, R.A., Bandi, P., Sauer, A.G., . . . Silvestri, G.A. (2021). State variation in low-dose computed tomography scanning for lung cancer screening in the united states. *JNCI: Journal of the National Cancer Institute*, *113*(8), 1044-1052.
- Greenspan, H., Van Ginneken, B., & Summers, R.M. (2016). Guest editorial deep learning in medical imaging: Overview and future promise of an exciting new technique. *IEEE transactions on medical imaging*, *35*(5), 1153-1159.
- Guo, Y., Feng, Y., Sun, J., Zhang, N., Lin, W., Sa, Y., & Wang, P. (2014). Automatic lung tumor segmentation on pet/ct images using fuzzy markov random field model. *Computational and mathematical methods in medicine*, 2014.
- Gupta, B., & Tiwari, S. (2014). Lung cancer detection using curvelet transform and neural network. *International Journal of Computer Applications*, *86*(1).
- Gurcan, M.N., Sahiner, B., Petrick, N., Chan, H.P., Kazerooni, E.A., Cascade, P.N., & Hadjiiski, L. (2002). Lung nodule detection on thoracic computed tomography images: Preliminary evaluation of a computer - aided diagnosis system. *Medical Physics*, *29*(11), 2552-2558.
- Hamedianfar, A., Mohamedou, C., Kangas, A., & Vauhkonen, J. (2022). Deep learning for forest inventory and planning: A critical review on the remote sensing approaches so far and prospects for further applications. *Forestry*, *95*(4), 451-465.
- Han, G., Liu, X., Zhang, H., Zheng, G., Soomro, N.Q., Wang, M., & Liu, W. (2019). Hybrid resampling and multi-feature fusion for automatic recognition of cavity imaging sign in lung ct. *Future Generation Computer Systems*, *99*, 558-570.
- Highamcatherine, F., & Highamdesmond, J. (2019). Deep learning. *SIAM Rev*, *32*, 860-891.
- Jonas, D.E., Reuland, D.S., Reddy, S.M., Nagle, M., Clark, S.D., Weber, R.P., . . . Armstrong, C. (2021). Screening for lung cancer with low-dose computed tomography: Updated evidence report and systematic review for the us preventive services task force. *Jama*, *325*(10), 971-987.
- Kaggle. KDSB (2017). Data Science Bowl 2017 lung Cancer Detection (dsb3).
- Kuruvilla, J., & Gunavathi, K. (2014). Lung cancer classification using neural networks for ct images. *Computer methods and programs in biomedicine*, *113*(1), 202-209.
- Liang, H., Hu, M., Ma, Y., Yang, L., Chen, J., Lou, L., . . . Xiao, Y. (2023). Performance of deep-learning solutions on lung nodule malignancy classification: A systematic review. *Life*, *13*(9), 1911.
- Ma, L., Wan, C., Hao, K., Cai, A., & Liu, L. (2023). A novel fusion algorithm for benign-malignant lung nodule classification on ct images. *BMC Pulmonary Medicine*, *23*(1), 474.
- Mandal, M., & Vipparthi, S.K. (2021). An empirical review of deep learning frameworks for change detection: Model design, experimental frameworks, challenges and research needs. *IEEE Transactions on Intelligent Transportation Systems*, *23*(7), 6101-6122.
- Masud, M., Muhammad, G., Hossain, M.S., Alhumyani, H., Alshamrani, S.S., Cheikhrouhou, O., & Ibrahim, S. (2020). Light deep model for pulmonary nodule detection from ct scan images for mobile devices. *Wireless Communications and Mobile Computing*, *2020*, 1-8.
- Nazir, I., AlQahtani, S.A., Jadoon, M.M., & Dahshan, M. (2023). Machine learning-based lung cancer detection using multiview image registration and fusion. *Journal of Sensors*, 2023.
- Ojala, T., Pietikäinen, M., & Harwood, D. (1996). A comparative study of texture measures with classification based on featured distributions. *Pattern recognition*, *29*(1), 51-59.
- Penedo, M.G., Carreira, M.J., Mosquera, A., & Cabello, D. (1998). Computer-aided diagnosis: A neural-network-based approach to lung nodule detection. *IEEE Transactions on Medical Imaging*, *17*(6), 872-880.
- Rao, P., Pereira, N.A., & Srinivasan, R. (2016). *Convolutional neural networks for lung cancer screening in computed tomography (ct) scans*. Paper presented at the 2016 2nd international conference on contemporary computing and informatics (IC3I).
- Ronneberger, O., Fischer, P., & Brox, T. (2015). *U-net: Convolutional networks for biomedical image segmentation*. Paper presented at the Medical Image

- Computing and Computer-Assisted Intervention–MICCAI 2015: 18th International Conference, Munich, Germany, October 5-9, 2015, Proceedings, Part III 18.
- Salama, W.M., Shokry, A., & Aly, M.H. (2022). A generalized framework for lung cancer classification based on deep generative models. *Multimedia Tools and Applications*, 81(23), 32705-32722.
- Shah, A.A., Malik, H.A.M., Muhammad, A., Alourani, A., & Butt, Z.A. (2023). Deep learning ensemble 2d cnn approach towards the detection of lung cancer. *Scientific Reports*, 13(1), 2987.
- Shen, D., Wu, G., & Suk, H.-I. (2017). Deep learning in medical image analysis. *Annual review of biomedical engineering*, 19, 221-248.
- Shen, S., Han, S.X., Aberle, D.R., Bui, A.A., & Hsu, W. (2019). An interpretable deep hierarchical semantic convolutional neural network for lung nodule malignancy classification. *Expert systems with applications*, 128, 84-95.
- Shimizu, R., Yanagawa, S., Monde, Y., Yamagishi, H., Hamada, M., Shimizu, T., & Kuroda, T. (2016). *Deep learning application trial to lung cancer diagnosis for medical sensor systems*. Paper presented at the 2016 International SoC Design Conference (ISOCC).
- Siegel, R.L., Miller, K.D., Wagle, N.S., & Jemal, A. (2023). Cancer statistics, 2023. *CA: a cancer journal for clinicians*, 73(1), 17-48.
- Soerjomataram, I., Cabaasag, C., Bardot, A., Fidler-Benaoudia, M.M., Miranda-Filho, A., Ferlay, J., . . . Znaor, A. (2023). Cancer survival in africa, central and south america, and asia (survcan-3): A population-based benchmarking study in 32 countries. *The Lancet Oncology*, 24(1), 22-32.
- Taher, F., & Sammouda, R. (2011). *Lung cancer detection by using artificial neural network and fuzzy clustering methods*. Paper presented at the 2011 IEEE GCC conference and exhibition (GCC).
- Tian, G., Fu, H., & Feng, D.D. (2008). *Automatic medical image categorization and annotation using lbp and mpeg-7 edge histograms*. Paper presented at the 2008 international conference on information technology and applications in biomedicine.
- Tong, G., Li, Y., Chen, H., Zhang, Q., & Jiang, H. (2018). Improved u-net network for pulmonary nodules segmentation. *Optik*, 174, 460-469.
- Wang, S., Chen, A., Yang, L., Cai, L., Xie, Y., Fujimoto, J., . . . Xiao, G. (2018). Comprehensive analysis of lung cancer pathology images to discover tumor shape and boundary features that predict survival outcome. *Scientific reports*, 8(1), 10393.